



Amylin Selectively Signals Onto POMC Neurons in the Arcuate Nucleus of the Hypothalamus

Thomas A. Lutz,¹ Bernd Coester,¹ Lynda Whiting,¹ Ambrose A. Dunn-Meynell,² Christina N. Boyle,¹ Sebastien G. Bouret,^{3,4} Barry E. Levin,⁵ and Christelle Le Foll¹

Diabetes 2018;67:805–817 | <https://doi.org/10.2337/db17-1347>

Amylin phosphorylates ERK (p-ERK) in the area postrema to reduce eating and synergizes with leptin to phosphorylate STAT3 in the arcuate (ARC) and ventromedial (VMN) hypothalamic nuclei to reduce food intake and body weight. The current studies assessed potential amylin and amylin-leptin ARC/VMN interactions on ERK signaling and their roles in postnatal hypothalamic pathway development. In amylin knockout mice, the density of agouti-related protein (AgRP)-immunoreactive (IR) fibers in the hypothalamic paraventricular nucleus (PVN) was increased, while the density of α -melanocyte-stimulating hormone (α MSH) fibers was decreased. In mice deficient of the amylin receptor components RAMP1/3, both AgRP and α MSH-IR fiber densities were decreased, while only α MSH-IR fiber density was decreased in rats injected neonatally in the ARC/VMN with an adeno-associated virus short hairpin RNA against the amylin core receptor. Amylin induced p-ERK in ARC neurons, 60% of which was present in POMC-expressing neurons, with none in NPY neurons. An amylin-leptin interaction was shown by an additive effect on ARC ERK signaling in neonatal rats and a 44% decrease in amylin-induced p-ERK in the ARC of leptin receptor-deficient and of ob/ob mice. Together, these results suggest that amylin directly acts, through a p-ERK-mediated process, on POMC neurons to enhance ARC-PVN α MSH pathway development.

Amylin is synthesized by pancreatic β -cells and is coreleased with insulin in response to eating and increasing glucose levels (1). The amylin receptor (AMY) is composed of the core calcitonin receptor (CTR) A or B (2), which heterodimerizes with

one or several receptor activity-modifying proteins (RAMP1, -2, and -3) (3,4). These components can be found in the area postrema (AP), nucleus of the solitary tract (NTS), the lateral hypothalamic area, ventromedial (VMN) and arcuate (ARC) hypothalamic nuclei, and the ventral tegmental area (5). Several studies have demonstrated that the AP is the primary site for amylin's satiating effects (6–8), but the ventromedial hypothalamus (VMH) (VMH = ARC + VMN) is also a direct target for amylin signaling. Diet-resistant (DR) rats whose CTR expression in the VMH was depleted displayed an increased weight and adiposity and insulin resistance, but high-fat diet intake was not affected compared with control rats (9), suggesting that VMH amylin signaling might directly control energy metabolism. In the VMH, amylin and leptin act synergistically to enhance STAT3-mediated leptin action and to decrease eating and weight gain (10–12). Amylin stimulates VMH microglial cells to secrete interleukin-6 (IL-6), which subsequently binds to its neuronal receptor coupled to gp130 to enhance leptin-induced pSTAT3 signaling (13,14).

In rodents, hypothalamic neurons are born during the 2nd week of gestation (15,16). However, the axonal connections between various hypothalamic nuclei only fully develop during the 2nd week postnatally in rodents (17). In the early postnatal period, endogenous leptin acts as a neurotrophic factor from postnatal day (P)4 to P12 whereby it stimulates axonal outgrowth from ARC α -melanocyte-stimulating hormone (α MSH) and agouti-related protein (AgRP) neurons to the hypothalamic paraventricular nucleus (PVN) (18). This process involves leptin's activation of ERK and STAT3 signaling pathways (19). Diet-induced obese (DIO) rats (20,21) are leptin resistant and have defective

¹Institute of Veterinary Physiology, University of Zurich, Zurich, Switzerland

²Veterans Affairs Medical Center, East Orange, NJ

³Developmental Neuroscience Program, The Saban Research Institute, Children's Hospital Los Angeles, Department of Pediatrics, University of Southern California, Los Angeles, CA

⁴INSERM U1172, Jean-Pierre Aubert Research Center, Lille, France

⁵Department of Neurology, Rutgers New Jersey Medical School, Newark, NJ

Corresponding author: Christelle Le Foll, christelle.lefoll@uzh.ch.

Received 8 November 2017 and accepted 9 February 2018.

This article contains Supplementary Data online at <http://diabetes.diabetesjournals.org/lookup/suppl/doi:10.2337/db17-1347/-/DC1>.

© 2018 by the American Diabetes Association. Readers may use this article as long as the work is properly cited, the use is educational and not for profit, and the work is not altered. More information is available at <http://www.diabetesjournals.org/content/license>.

ARC α MSH and AgRP axonal outgrowth to the PVN that persists into adulthood (21). Amylin treatment of DIO neonates from P0 to P16 partially improves impaired ARC leptin signaling and enhances defective α MSH and AgRP ARC-PVN axonal fiber development (22).

ERK signaling pathway activation leads to the phosphorylation of ERK1/2 (p-ERK) (23,24) and activation of gene transcription and also triggers rapid neuronal responses by directly modulating neuronal activity (25,26). Amylin's activation of the ERK1/2 pathway in the AP is neuron specific and is colocalized with CTR-expressing neurons (27), and their activation is correlated with a decrease in eating. ERK signaling can also be activated by leptin in the ARC, which decreases eating and weight gain and increases thermogenic sympathetic outflow (28).

This study aims to determine the role of endogenous amylin as a neurotrophic factor in the ARC using various rodent models lacking amylin or AMY signaling. Next, we assessed whether amylin activates ERK signaling in specific ARC and VMN neurons and whether amylin signaling was dependent upon leptin signaling. Finally, we examined whether the hindbrain was required for amylin to act on ARC neurons.

RESEARCH DESIGN AND METHODS

Animal Husbandry and Diet

Animals were maintained in a temperature-controlled ($21 \pm 2^\circ\text{C}$) room on a 12:12 h light:dark schedule. Standard chow (category no. 3430, energy content 3.15 kcal/g; Provimi Kliba, Kaiseraugst, Switzerland) and water were provided ad libitum. Animals were handled and housed in an enriched environment. Male and female mice were used and included in the study when no differences between the sexes were noticed. All procedures were approved by the Veterinary Office of the Canton Zurich (no. 029/2015) and the Institutional Animal Care and Use Committee of the East Orange Veterans Affairs Medical Center.

Amylin Signaling in NPY-hrGFP, LepRb LoxTB, RAMP 1/3 Knockout, and Amylin Knockout Mice

NPY-hrGFP [B6.FVB-Tg(Npy-hrGFP)1Lowl/J, no. 006417; The Jackson Laboratory], LepRb LoxTB [B6.129X1(FVB)-LepRtm1Jke/J, no. 019111; The Jackson Laboratory], and wild-type (WT) littermates were bred in our facility. LepRb LoxTB mice possess a transcription blocker cassette that prevents the transcription of the LepRb gene (29). NPY-hrGFP mice allow the identification of NPY neurons without any additional immunohistochemistry (IHC) staining owing to their endogenous GFP fluorescence driven by the NPY promoter. Male and female NPY-hrGFP and LepRb LoxTB mice and respective WT littermates were fasted for 6 h and, at dark onset, injected with saline (NaCl 0.9%) versus amylin (50 $\mu\text{g}/\text{kg}$ i.p.; Bachem AG, Bubendorf, Switzerland) ($n = 8/\text{group}$) and 45 min later perfused with saline followed by 2% paraformaldehyde (PFA) in 0.1 mol/L phosphate buffer (pH 7.4).

Male RAMP1/3 double knockout (KO) mice (background: 129S6/SvEv [kindly donated by Kathleen Caron, University of South Carolina]) (30) and amylin KO (background: C57BL/6)

(12) were bred, and 6-week-old WT and KO littermates were injected at dark onset after a 6-h fast with either saline or amylin (50 $\mu\text{g}/\text{kg}$) ($n = 8/\text{group}$) and perfused with 4% PFA in borate buffer (pH 9.5). Brains were postfixed in 20% sucrose-4% PFA, cryoprotected overnight, and frozen.

Effect of Leptin Replacement From P4 to P16 in ob/ob Mice on Amylin Signaling

ob/+ mice (B6.Cg-Lepob/J Jax, no. 000632; Charles River Laboratories, Calco, Italy) were bred, and litters were culled to six to eight pups and genotyped at P2. WT pups and ob/ob pups were injected once daily with PBS or leptin (10 mg/kg s.c. in PBS; PeprTech, London, U.K.) from P4 to P16. At P24, mice were fasted and injected with amylin (i.p. 50 $\mu\text{g}/\text{kg}$) ($n = 4-7/\text{group}$) and were perfused similarly to amylin KO mice (Fig. 5I).

Effect of Neonatal Depletion of VMH Amylin Signaling in DR Rats on ARC-PVN Pathway Development

Male rats selectively bred to express the DR phenotype were used (20). DR litters were culled to six male and four female pups per dam at P2. At P4, one male from each litter was injected bilaterally in the VMH with adeno-associated virus (AAV) CTR short hairpin RNA (shRNA) (serotype 1 [0.25 μL saline containing 0.625 E8 genome copies]) and one male from the same litter was injected with AAV control (9,31,32). At P17, all rats were perfused with 4% PFA in borate buffer. AAV injection and fluorescence was verified under the microscope, and CTR depletion efficacy was previously validated in the VMH (9).

Amylin and Leptin Interaction in P12 and P13 Sprague-Dawley Rats

Four Sprague-Dawley dams with a P8 litter (Charles River Laboratories, Sulzfeld, Germany) were used. At P12 or P13, male and female rats were weighed and injected with saline, amylin (25 $\mu\text{g}/\text{kg}$ i.p.), leptin (2.5 mg/kg i.p.), or amylin + leptin ($n = 8/\text{group}$). Forty-five minutes after the injection, rats were sacrificed and brains were frozen on dry ice. The ARC was punched out of 300- μm slices and lysed (10 $\mu\text{L}/\text{mg}$ of tissue) as previously published (33). Protein (20 μg) was loaded onto a 12% TGX gel (Bio-Rad Laboratories, Munich, Germany) and transferred onto polyvinylidene fluoride membrane (Bio-Rad Laboratories). p-ERK (1:1,000, category no. 9101; Cell Signaling, BioConcept, Allschwill, Switzerland) antibody was applied to the membrane and detected using chemiluminescence following the manufacturer's protocol. The membrane was then stripped (200 mmol/L glycine, 3.5 mmol/L SDS, and 1% Tween 20, pH 2.2) for 20 min and reprobed after blocking with total ERK antibody (1:1,000, category no. 9102; Cell Signaling). Images were acquired using the LAS-3000 Imager (Fujifilm), and the density of the immunoreactive (IR) bands was quantified (ImageJ) and the ratio (p-ERK/total ERK \times 100) was calculated for each rat.

Amylin Effect in Intact and AP-Lesioned Sprague-Dawley Rats

Thirty-six 7-week-old male Sprague-Dawley rats with an initial weight of 200–250 g (Janvier Labs, Le Geneste-Saint-Isle,

France) were used. On the day of sacrifice, the rats were fasted for 4 h and injected with saline versus amylin (50 $\mu\text{g}/\text{kg}$ i.p.) at dark onset. Five, 15, or 45 min later, rats were perfused to assess ERK signaling.

Further, sixteen 250-g male Sprague-Dawley rats were anesthetized and AP lesion was performed as previously published (34,35). For confirmation of the AP lesion, rats underwent an amylin-induced anorexia test where amylin (20 $\mu\text{g}/\text{kg}$ i.p.) and saline were injected at dark onset after a 12-h fast and eating was measured at 1 h, 2 h, and 24 h. On the day of the sacrifice, rats were fasted for 6 h, injected with amylin (50 $\mu\text{g}/\text{kg}$), and perfused 45 min later with saline followed by 4% PFA in phosphate buffer ($n = 6/\text{group}$). The brains were postfixed overnight, cryoprotected, and frozen.

IHC

p-ERK and POMC IHC

Brains were sectioned serially at 25 μm through the ARC and VMN (36) and slide mounted onto Superfrost Plus slides (Life Technologies Europe, Zug, Switzerland). Single-label p-ERK IHC was carried out as previously described using rabbit anti-p-ERK antibody (1:1,000) (27,37). Double-labeled p-ERK-POMC IHC was carried out subsequently (22) by incubating sections for 72 h with rabbit anti-POMC antibody (1:1,000, category no. H-029-30; Phoenix Pharmaceuticals, Karlsruhe, Germany) and Alexa Fluor 488 goat anti-rabbit for 2 h (1:250; Life Technologies) and cover-slipped using VECTASHIELD HardSet mounting medium (Vectorlabs, Servion, Switzerland).

αMSH and AgRP IHC

αMSH and AgRP IHC were performed using previously described methods (21,22,38). Brains were sectioned at 25 μm serially through the PVN and dorsomedial nucleus (DMN). For αMSH , sections were incubated after overnight blocking (0.3% Triton and 2% normal donkey serum in potassium PBS) with sheep anti- αMSH (1:40,000, category no. ab5087; Merck Millipore, Schaffhausen, Switzerland) for 72 h and visualized with Alexa Fluor 488 donkey anti-sheep secondary antibody (1:200). For AgRP, sections were incubated with rabbit anti-AgRP (1:4,000, category no. H-003-57; Phoenix Biotech) for 72 h. The signal was amplified using a TSA Biotin Tyramide kit (NEL700A001KT; PerkinElmer, Rodgau, Germany) and visualized with streptavidin-Alexa Fluor 488 conjugate (1:1,000).

CTR IHC

Sections were blocked for 90 min with 3% normal donkey serum and 0.3% Triton in 0.1 mol/L PBS. Slides were washed and incubated for 48 h at 4°C in rabbit anti-CTR (1:1,000, category no. ab11042; Abcam, Cambridge, U.K.) followed by CY3 donkey anti-rabbit (1:200; Jackson ImmunoResearch) for 2 h (27).

Quantitative Analysis of Immunolabeled Cells and Fibers

Cells expressing p-ERK and POMC in the ARC, VMN, AP, and NTS were imaged using an L2 Imager upright microscope (Zeiss Germany). For quantitative analysis of αMSH

and AgRP fiber densities, three sections through the PVN and DMN from animals of each experimental group were acquired using a Zeiss SP8 confocal system equipped with a 20 \times /0.75 objective (HD1 488, laser 2% with 10% gain, zoom 1, pinhole 1, Z-stack 21 μm , and step of 1.5 μm). Slides were numerically coded to obscure the treatment group. Image analysis was performed using ImageJ analysis software (National Institutes of Health) as previously described (22,37). For representative images, images were equally adjusted for brightness and contrast within the same experiment.

Statistics

Statistical comparisons among variables were made by one- or two-way ANOVA, as appropriate, with Bonferroni post hoc analysis. Comparisons between control and amylin-treated groups were assessed using *t* test for nonparametric statistics (GraphPad Prism, La Jolla, CA). All data are expressed as mean \pm SEM.

RESULTS

Endogenous Amylin Acts as a Neurotrophic Factor on ARC Neurons

Exogenous amylin enhances leptin's neurotrophic action on AgRP and αMSH ARC-PVN axon fiber development during the early postnatal period of selectively bred DIO rats (22). To assess the potential endogenous amylin neurotrophic action in the hypothalamus, we used different models where amylin or components of AMY were absent. In 6-week-old male amylin KO, AgRP-IR fiber density in the PVN was increased by 46%, while αMSH -IR fiber density was decreased by 26% ($P < 0.05$) (Fig. 1A, B, and G) compared with respective WT littermates. In 6-week-old male RAMP1/3 KO mice, AgRP- and αMSH -IR fiber density was decreased by 51% and 37% compared with WT mice, respectively ($P < 0.05$) (Fig. 1C, D, and H). In selectively bred DR rats injected in the VMH at P4 with an AAV CTR shRNA, AgRP-IR fibers analyzed at P17 were unaffected, whereas αMSH -IR PVN fiber density was decreased by 48% compared with AAV controls ($P < 0.05$) (Fig. 1E, F, and I). Finally, AgRP and αMSH -IR fiber densities were similar to WT littermates in the DMN of amylin KO and RAMP1/3 KO mice (Supplementary Fig. 1).

Amylin Activates ERK Signaling in ARC POMC Neurons of Adult Rodents

The time course of amylin-induced p-ERK in the median eminence (ME), ARC, and VMN was determined in 7-week-old male Sprague-Dawley rats (Supplementary Fig. 2). Amylin significantly activated ERK signaling at 5 min and 45 min but not at 15 min in the ME, ARC, and VMN (Supplementary Fig. 2 and Fig. 2A and B). At 45 min, amylin increased the number of p-ERK-positive neurons by 70% and 174% in the ARC and the VMN, respectively ($P < 0.05$) (Fig. 2A and B). Since the total number of p-ERK-positive neurons was 8–10 times higher in the ARC than in the VMN, the following experiments focused on the ARC. Amylin administration increased the total number of p-ERK-expressing ARC neurons by 47%. The total number of POMC-positive neurons was

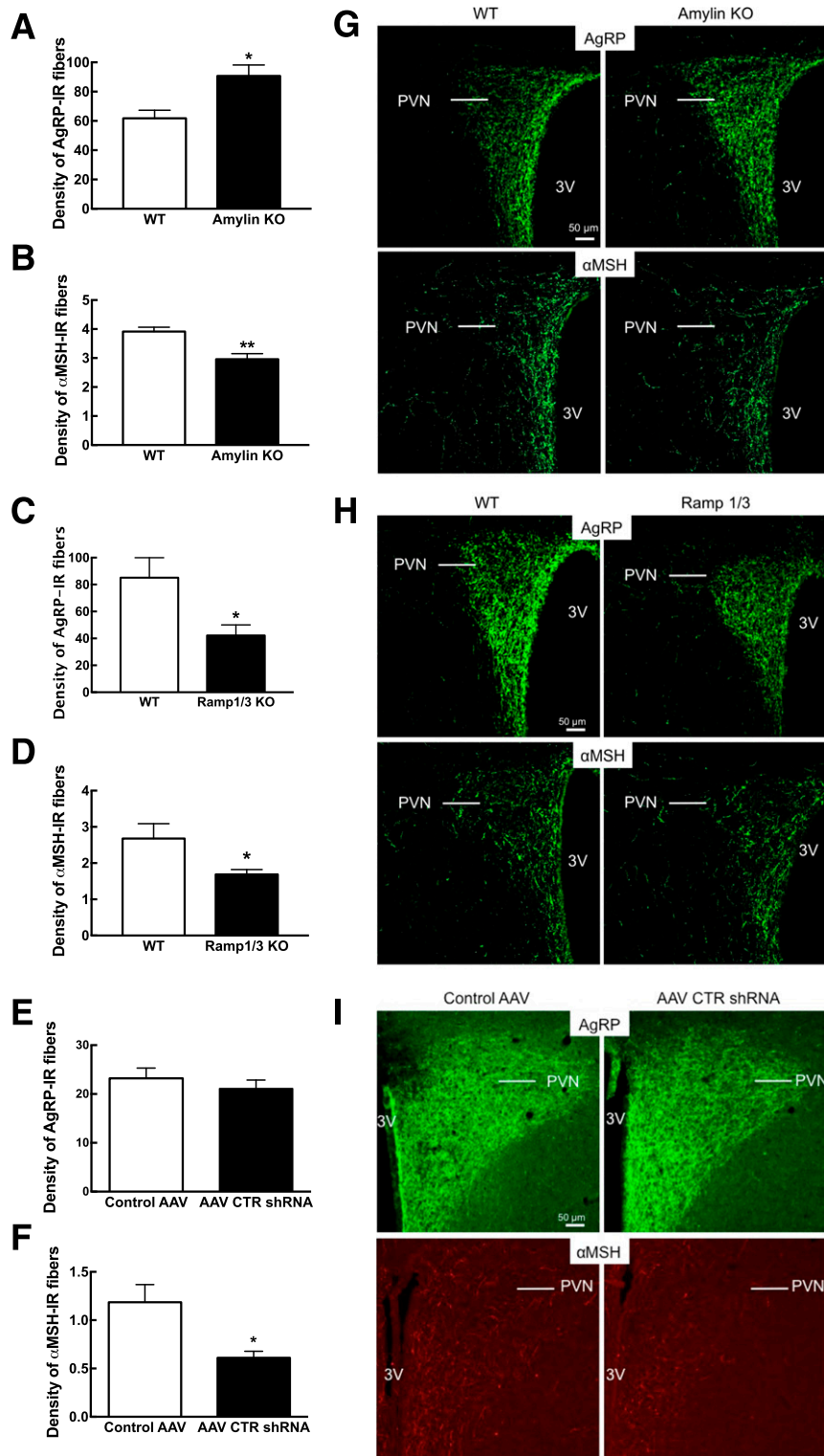


Figure 1—AgRP (A, C, and E) and α MSH (B, D, and F) PVN were stained and axonal density was quantified in 6-week-old male amylin KO and Ramp1/3 KO mice and their respective WT controls, and male DR rats were injected in the ARC and VMN at P4 with control vs. AAV CTR shRNA. G–I: Representative images of AgRP-IR fibers and α MSH-IR fibers in the PVN for each animal model. The staining and quantification of the amylin KO and Ramp1/3 KO mice and DR rats were done independently. $N = 8$ /group. Data are expressed as mean \pm SEM. * $P < 0.05$ and ** $P < 0.01$ vs. WT mice after Student t test. 3V, third ventricle.

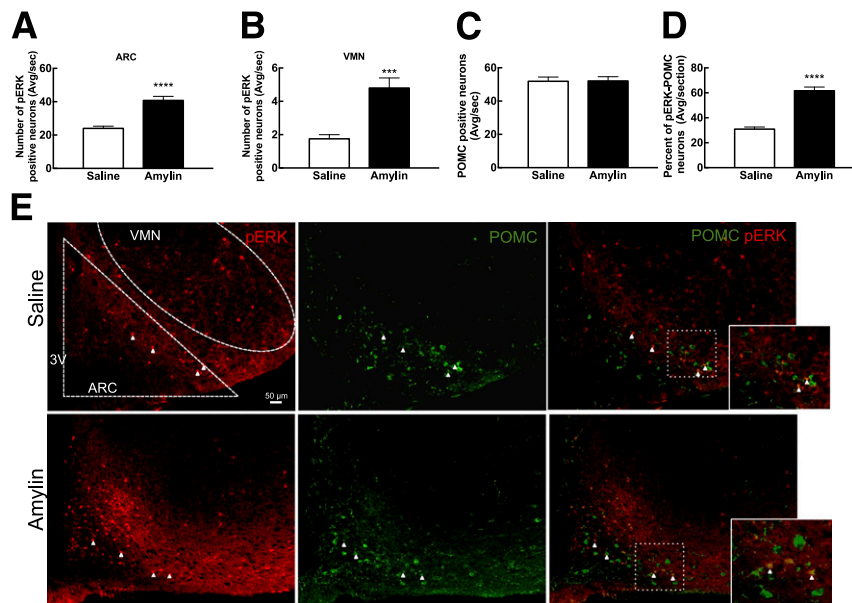


Figure 2—Amylin-induced p-ERK neurons in the ARC (A) and VMN (B) of 7-week-old male Sprague-Dawley rats ($n = 6/\text{group}$) 45 min after saline or amylin injection ($50 \mu\text{g}/\text{kg}$ i.p.). Neurons were also double labeled for POMC. C: Number of POMC neurons quantified in the ARC. D: Percentage of p-ERK-activated POMC neurons. E: $20\times$ representative picture of the ARC after saline and amylin injection. p-ERK neurons are in red and POMC neurons in green. The white arrows represent the double-labeled neurons. Data are means \pm SEM with average neuronal count per section. **** $P < 0.0001$ and *** $P < 0.001$ vs. saline-treated rats after Student t test. 3V, third ventricle; Avg/sec, average per section.

unaltered, but amylin doubled the number of POMC-positive neurons that coexpressed p-ERK compared with controls ($P < 0.0001$) (Fig. 2C and D). On the other hand, there was no effect of amylin on the percentage of NPY neurons that expressed p-ERK (Fig. 3). Thus, amylin increased overall ARC p-ERK expression selectively in POMC as opposed to NPY neurons. In addition, amylin also activated ERK signaling in the ME and VMN but to a markedly lesser degree than in the ARC.

RAMP1/3 KO Mice Are Insensitive to ERK Signaling Activation

Similarly to results in outbred rats (Fig. 2), amylin increased ERK phosphorylation in the ARC of WT mice by 61% ($P <$

0.01), while amylin had no effect in RAMP1/3 KO mice (Fig. 4A and D). The depletion of RAMP1 and -3 had no effect on the number of POMC neurons (Fig. 4C), but while amylin increased p-ERK signaling in POMC neurons by 85% in WT mice ($P < 0.05$), it had no effect in the RAMP1/3 KO mice (Fig. 4B and D). This suggests that functional amylin receptors (AMY1 or AMY3 [39]) are necessary for amylin to increase ERK phosphorylation in the ARC.

Amylin-Induced p-ERK in the ARC of Leptin- and LepRb-Deficient Mice

Since amylin and leptin signaling in the hypothalamus are closely linked (9,12,13), amylin-induced p-ERK was first assessed in leptin receptor-deficient (LepRb LoxTB) mice.

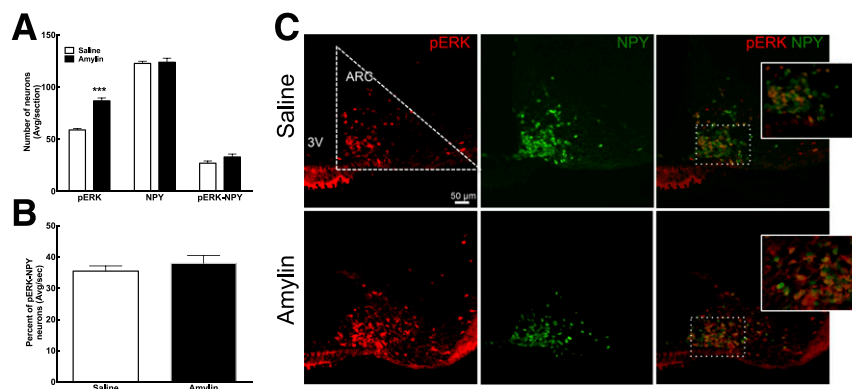


Figure 3—Male and female 4-week-old NPY-hrGFP mice were tested for ARC amylin response. A: ARC amylin-induced p-ERK 45 min after saline or amylin injection ($50 \mu\text{g}/\text{kg}$ i.p.). B: Percentage of p-ERK-activated NPY neurons. C: $20\times$ representative picture of the ARC after saline or amylin injection. p-ERK neurons are in red, and NPY-hrGFP neurons are in green. $N = 8/\text{group}$. Data are means \pm SEM. *** $P < 0.001$ vs. saline-treated rats after Student t test. 3V, third ventricle; Avg/sec, average per section.

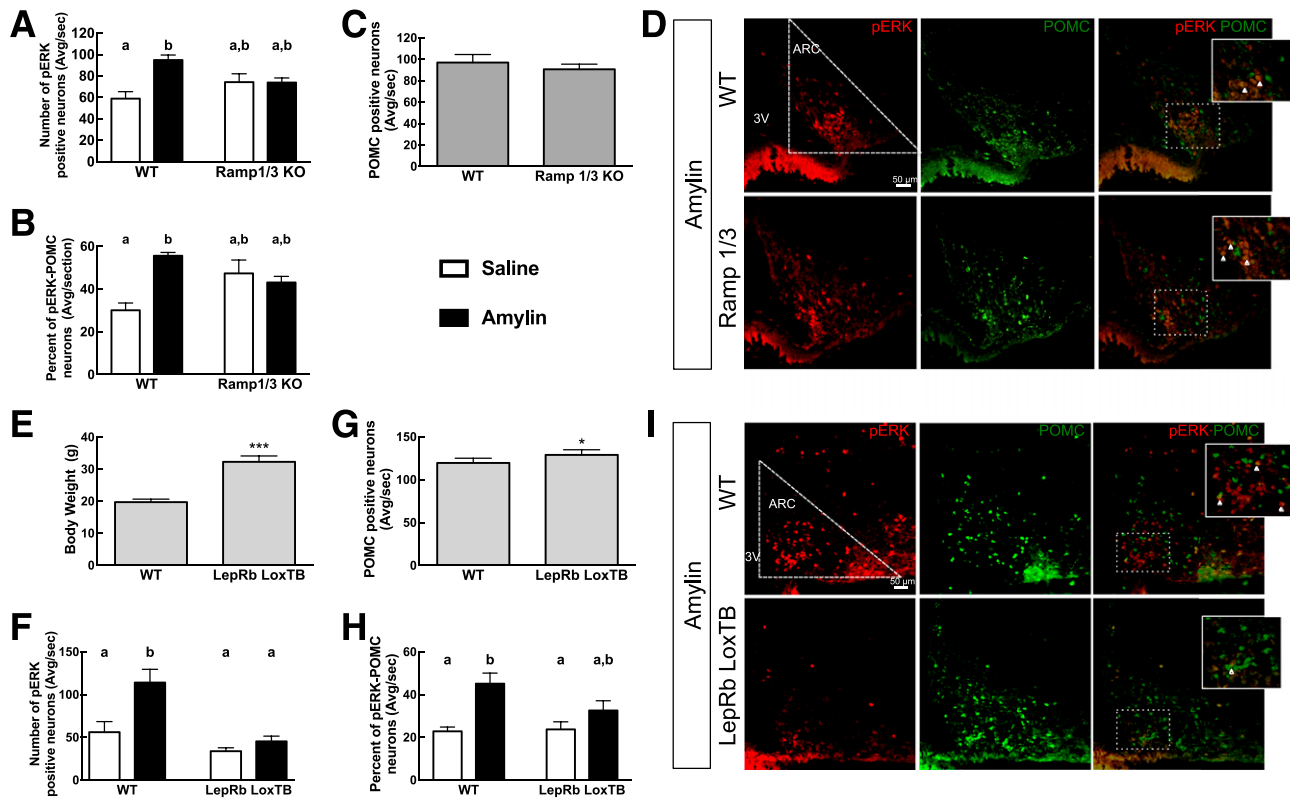


Figure 4—Male 6-week-old Ramp1/3 KO and male and female 7-week-old LepRb LoxTB mice and their respective WT littermates were tested for ARC amylin response. **A:** ARC amylin-induced p-ERK 45 min after saline or amylin injection (50 μ g/kg i.p.) in Ramp1/3 KO mice. Neurons were also double labeled for POMC. **B:** Percentage of p-ERK-activated POMC neurons. **C:** Number of POMC neurons quantified in the ARC. **D:** 20 \times picture of p-ERK and POMC IHC in WT and Ramp1/3 KO mice injected with amylin. p-ERK neurons are in red, and POMC neurons are in green. White arrows represent the double-labeled neurons. **E:** Weight at sacrifice in LepRb LoxTB mice. **F:** ARC amylin-induced p-ERK 45 min after saline or amylin injection (50 μ g/kg i.p.) in LepRb LoxTB mice. Neurons were also double labeled for POMC. **G:** Number of POMC neurons quantified in ARC. **H:** Percentage of p-ERK-activated POMC neurons. **I:** 20 \times picture of p-ERK and POMC IHC in WT and LepRb LoxTB mice injected with amylin. p-ERK neurons are in red, and POMC neurons are in green. The white arrows represent the double-labeled neurons. $N = 8$ /group. Data are means \pm SEM. * $P < 0.05$ and *** $P < 0.01$ vs. WT mice after Student t test. Parameters with differing lowercase letters differ from each other at the $P < 0.05$ level by post hoc Bonferroni adjustment after significant intergroup differences were found by one-way ANOVA. 3V, third ventricle; Avg/sec, average per section.

At 7 weeks of age, LepRb LoxTB mice weighed almost twice as much as WT littermates ($P < 0.05$) (Fig. 4E); amylin increased ARC p-ERK by 103% in WT mice ($P < 0.05$) but not in LepRb LoxTB mice (Fig. 4F and I). Unexpectedly, LepRb LoxTB mice had a slightly increased number of POMC neurons compared with WT mice (7% [$P < 0.05$]) (Fig. 4G and I). More importantly, while amylin doubled the number of POMC neurons that coexpressed p-ERK in WT mice ($P < 0.05$), it had no such effect in the LepRb LoxTB mice (Fig. 4H and I).

This suggests a critical interaction between leptin signaling and amylin-induced ERK phosphorylation in adult POMC neurons. Since LepRb LoxTB mice and leptin-deficient ob/ob mice both have defective ARC-PVN axonal pathway development (18,40), we next assessed the potential role of amylin-leptin signaling interactions on this defective development. ob/ob mice and WT littermates were treated once daily with leptin or saline from P4 to P16 (18). Leptin treatment decreased weight gain at P16 in WT and ob/ob mice by 39% and 40%, respectively, compared with WT

and ob/ob saline-treated mice ($P < 0.05$) (Fig. 5B). However, by the time of sacrifice, i.e., 8 days after the cessation of leptin treatment, ob/ob leptin-treated mice displayed the same weight gain as ob/ob saline-treated mice (Fig. 5B). As expected from previous studies (18), PVN α MSH-IR fiber density was decreased by 38% in ob/ob saline-treated mice compared with WT mice ($P < 0.05$) (Fig. 5C and D), whereas leptin restored α MSH-IR fiber density in ob/ob leptin-treated mice to the level of WT littermates ($P < 0.05$) (Fig. 5C and D). The number of amylin-induced ARC p-ERK neurons in ob/ob saline-treated mice was reduced by 46% compared with WT mice but was restored to WT levels after neonatal leptin treatment ($P < 0.05$) (Fig. 5E and H). The total number of POMC neurons was similar in WT and ob/ob mice (Fig. 5F and H), but the number of POMC neurons in which amylin induced p-ERK was decreased by 48% in ob/ob saline-treated mice compared with WT mice ($P < 0.05$) (Fig. 5G and H). p-ERK was restored to control levels in leptin-treated ob/ob mice ($P < 0.05$) (Fig. 5G and H). Leptin treatment in WT mice had no effect on α MSH-IR

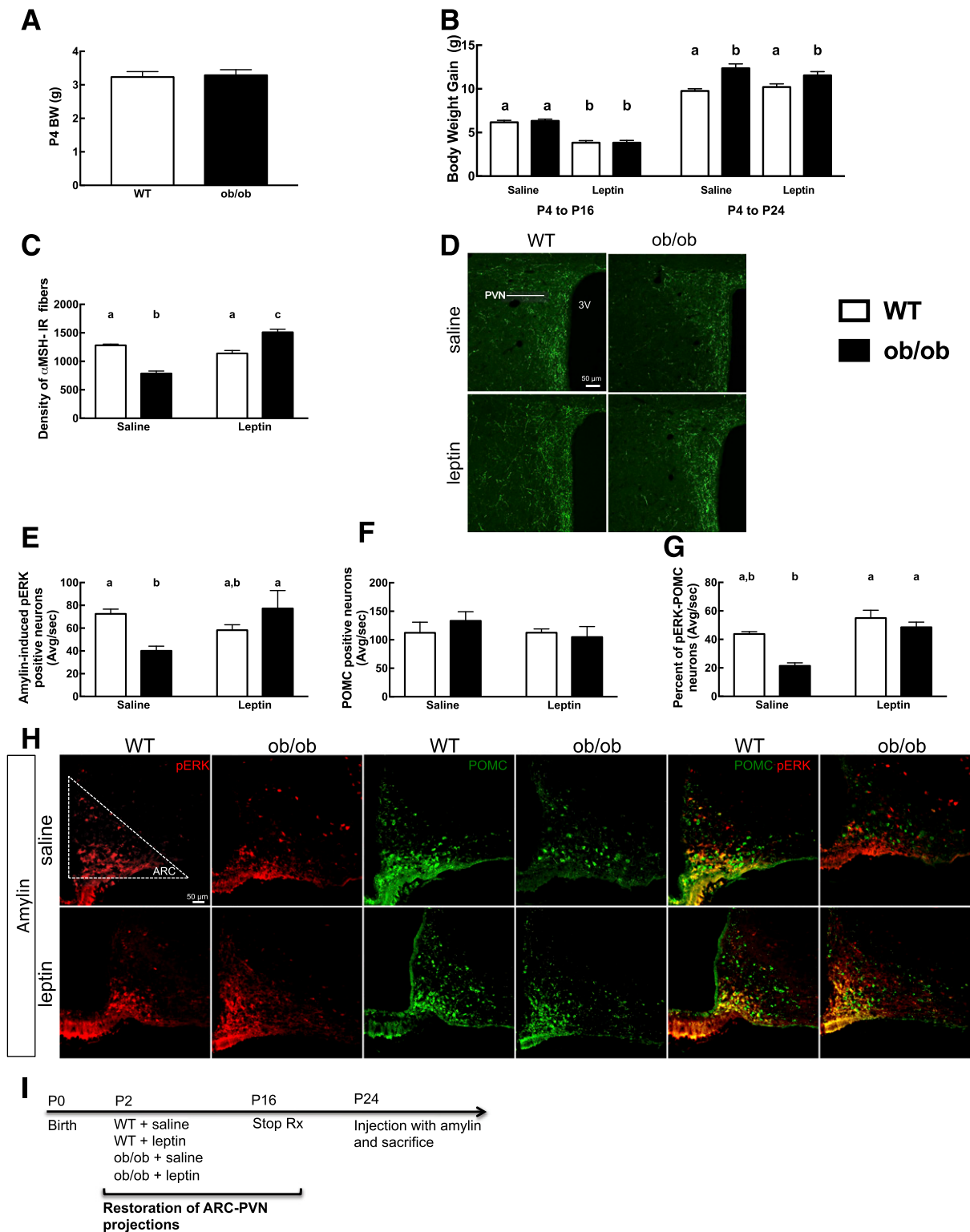


Figure 5—Amylin-induced p-ERK in ARC of WT vs. leptin-deficient (ob/ob) mice. ob/ob and WT mice were treated with leptin (10 mg/kg s.c.) or saline from P4 to P16. Mice were injected at P24 with amylin (50 μ g/kg i.p.) and sacrificed 45 min later. Weight at P4 (A) and weight gain during the treatment time (P4 to P16) and at the time of sacrifice at P24 (B). α -MSH PVN axonal density at P24 (C) and 20 \times confocal stack representative picture of the PVN area (D). E: Amylin-induced p-ERK neuronal count in the ARC. Neurons were also double labeled for POMC. F: Number of POMC neurons quantified in the ARC. G: Percentage of p-ERK-activated POMC neurons. H: 20 \times picture of p-ERK and POMC IHC in WT and ob/ob mice treated with saline or leptin after amylin injection. p-ERK neurons are in red, and POMC neurons are in green. I: Timeline of the experiment. *N* = 4–7/group. Data are means \pm SEM. Parameters with differing lowercase letters differ from each other at the *P* < 0.05 level by post hoc Bonferroni adjustment after significant intergroup differences were found by one-way ANOVA. 3V, third ventricle; Avg/sec, average per section; BW, body weight; Stop Rx, stop treatment.

fiber density or p-ERK or POMC neurons (Fig. 5C–G). Thus, intact leptin signaling is required for the ability of amylin to activate ERK phosphorylation and to support normal ARC-PVN axonal outgrowth in POMC neurons.

Amylin and Leptin Coactivate ERK Signaling in the ARC of Neonatal Rats

While we showed that amylin-induced ERK signaling is codependent with leptin signaling, we next assessed the effect of amylin and leptin on p-ERK in the ARC of neonatal rats during the period when their ARC-PVN neuronal pathways are developing. P12 male and female rats were injected with subthreshold doses of amylin, leptin, or amylin+leptin at dark onset. Single injection of amylin or leptin did not activate ERK in the ARC, whereas their combination increased p-ERK signaling by 57% ($P < 0.05$) (Fig. 6). This suggests that both amylin and leptin coactivate ERK signaling in neonatal animals in an additive manner that might explain their neurotrophic interactions in outgrowth of ARC POMC axons to the PVN.

Amylin Signaling in the ARC and VMN Is Independent of Its AP Actions

As the AP is thought to be the primary site of peripheral amylin's satiating action (6,8) and since the amylin activation pathway projects to the lateral parabrachial nucleus, which then projects densely to the ARC and VMN (41), it is possible that amylin acts indirectly on ARC neurons through this polysynaptic pathway. Thus, AP-lesioned rats were assessed for amylin-induced p-ERK in the ARC and VMN. As expected, AP-lesioned rats lost weight and decreased their eating compared with sham-lesioned rats (Fig. 7A and B). As published previously (34,35), sham rats ate less 1 h and 2 h after amylin injection, while AP-lesioned rats were insensitive to the anorectic effect of peripheral amylin (Fig. 7C and D). Nevertheless, amylin-induced p-ERK in the ARC and VMN was similar in sham- and AP-lesioned rats (Fig. 7E–G), suggesting that amylin acts directly in those nuclei to activate ERK signaling. We have to mention here that p-ERK signaling was not directly compared between saline-injected AP-lesioned versus sham-lesioned rats, thus creating a limitation to our conclusion. However, we do not expect a differential effect of saline in these animals because we have previously published studies examining the effect of AP lesions on amylin-induced cFos in the NTS, which is the direct downstream target, and we have never found any difference between sham- and AP-lesioned saline-injected animals (34,42).

DISCUSSION

These studies highlight the role of amylin signaling in the VMH and show, for the first time, that amylin activates ERK signaling in the ARC and that this activation occurs preferentially in POMC versus NPY/AgRP neurons. Although exogenous amylin exerts a neurotrophic effect on axonal outgrowth of both POMC and NPY/AgRP neurons (22), we show here that endogenous amylin directly exerts

neurotrophic properties specifically on POMC neurons, presumably via p-ERK signaling. On the other hand, amylin's neurotrophic effect on NPY/AgRP neurons appears to be indirect, possibly via IL-6 signaling (13,22). Furthermore, in neonatal and adult rodents, exogenous amylin activated the p-ERK signaling pathway selectively in ARC POMC neurons, and this activation was leptin dependent. Importantly, we show for the first time that leptin and LepRb are both necessary for amylin to activate ARC ERK signaling and that amylin and leptin exert an additive activation of VMH ERK signaling. Finally, we demonstrated that amylin hypothalamic signaling is independent of input coming from the AP, amylin's suggested primary site of action for its satiating effect (6,8).

The neurotrophic action of endogenous amylin was demonstrated using different rodent models where amylin signaling was disrupted. Amylin KO and RAMP1/3 KO mice and rats depleted of CTR in the VMH all displayed decreased POMC (α MSH) axonal projections to the PVN. AgRP fiber density was decreased in RAMP1/3 KO mice but was unaffected in DR rats depleted of CTR in the VMH. We thus hypothesize that endogenous amylin might act directly on POMC neurons through ERK signaling to enhance α MSH axonal fiber outgrowth, whereas it acts indirectly on NPY/AgRP neurons, probably by first acting on microglial cells to increase IL-6 production, which then enhances leptin-induced p-STAT3 to increase NPY/AgRP axonal fiber outgrowth (13,22) (Fig. 8). This hypothesis is supported by the fact that IL-6 KO mice only showed a decrease in AgRP and not in α MSH PVN fiber density (22). One important caveat of this study is that the assessment of fiber density using IHC does not necessarily correlate with axonal outgrowth, since the amount of AgRP and α MSH peptide can vary depending upon both the density of fibers and the turnover of the peptide at the axon terminal (43). However, the advantage of using IHC is that we are able to distinguish between the fibers carrying specific neuropeptides (21). While AgRP axons in the PVN arise only from the ARC (44) and arise mostly from NPY/AgRP neurons (44,45), NPY axons in the PVN can additionally arise from hindbrain NPY neurons (46). Thus, AgRP staining represents a reasonable means of identifying axons arising from NPY/AgRP ARC neurons.

Surprisingly, in amylin KO mice, AgRP PVN axonal fiber density was increased, whereas it was decreased in RAMP1/3 KO mice. Since these mice had either no amylin or no AMY signaling, respectively, we would have expected the same outcome. It is possible that some of amylin's effect on NPY/AgRP neurons might still be present in RAMP 1/3 KO mice, since they still have the functional RAMP2 subunit and amylin could thus act through this receptor subtype. RAMP2 has the lowest affinity for amylin compared with RAMP1 and -3 (39,47); thus, RAMP2 might be sufficient to maintain amylin's neurotrophic effect during the neonatal period but not during adulthood, as shown by the decrease in ERK phosphorylation after amylin injection. Unfortunately, this hypothesis cannot be tested directly owing to the lethality of RAMP2 KO (48). Aside from amylin, AMY1, -2, and -3 are also the target of other peptides such

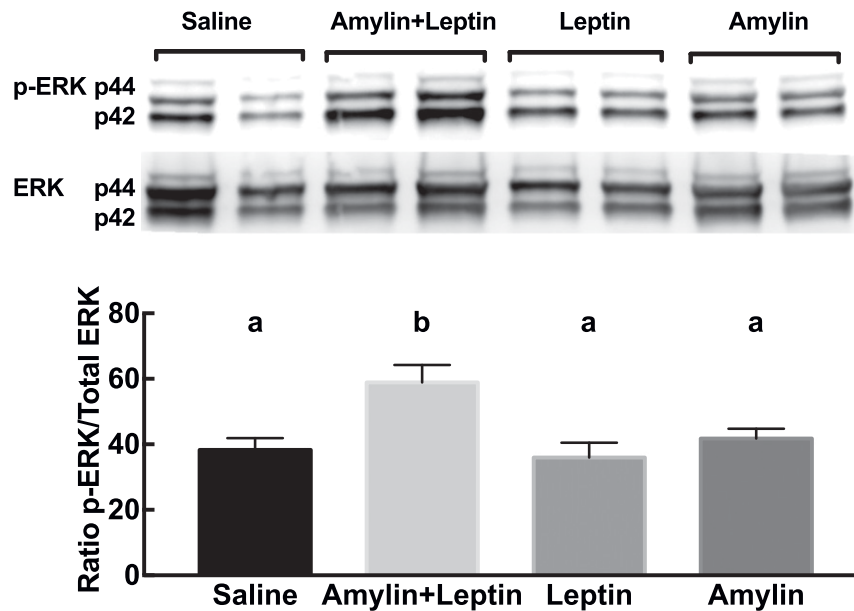


Figure 6—p44/42 p-ERK and total p44/42 ERK1/2 in the ARC of P12 rats 45 min after saline, amylin (25 μ g/kg i.p.), leptin (2.5 mg/kg i.p.), or amylin+leptin injection. Data are represented as the ratio of p-ERK to total ERK. $n = 8$ /group. Data are means \pm SEM. Parameters with differing lowercase letters differ from each other at the $P < 0.05$ level by post hoc Bonferroni adjustment after significant intergroup differences were found by one-way ANOVA.

as CGRP. In particular the AMY1 has been claimed to be a second CGRP receptor, even though CGRP has a lower affinity for these receptors than amylin (39). Thus, the depletion of RAMP1/3 could alter a possible CGRP neurotrophic action on NPY/AgRP neurons while remaining intact in amylin KO mice. Last, this difference of effect on AgRP PVN fibers could also result from the fact that amylin KO and RAMP1/3 KO mice are bred on different backgrounds (C57BL/6 vs. 129Sv) (49). Overall, these studies strongly suggest that endogenous amylin secreted by the pancreas or locally by neurons (50) is necessary for the full development of neuronal connections among hypothalamic nuclei during the neonatal period in rodents. However, the exact time period by which amylin exerts its neurotrophic action during the formation of the ARC-PVN pathways remains to be determined. It is known that postnatal amylin levels are similar to levels in adult animals and there is no amylin “surge” similar to that seen for leptin between P6 and P10 (51). Also, amylin is cosecreted with insulin by the pancreatic β -cells, and insulin secretion starts at embryonic day 12 and increases progressively until birth (52). Finally, amylin administration from P4 to P16 corrects the leptin resistance of selectively bred DIO rats and, as a consequence, corrects their defective ARC-PVN α MSH and AgRP projections (22).

Finally, our studies suggest that endogenous amylin acts as a neurotrophic factor directly and preferentially on POMC neurons, while its neurotrophic effect on NPY/AgRP neurons appears to be indirect, possibly via microglial IL-6 production (13,22). While we believe that the action of postnatal amylin on POMC neurons versus NPY/AgRP

neurons is well established, it is important to mention here that it has recently been shown that 25% of POMC neurons also express AgRP (53) and that half of embryonic POMC-expressing precursors adopt a non-POMC fate at adulthood. Moreover, nearly one-quarter of the mature NPY-positive cell population shares a common progenitor with POMC-positive cells (15).

We next examined amylin signaling in adult animals using p-ERK as a specific marker for amylin activation of the ERK signaling pathway. In the AP, amylin directly activates the ERK signaling pathway, which was shown to correlate with an amylin-induced decrease in eating (27). Here, we demonstrated that amylin stimulates p-ERK signaling primarily in the ARC, where it activates 8–10 times more neurons than in the VMN or ME. On the other hand, amylin’s sensitizing effect on leptin signaling is more potent in the VMN, with a greater activation of p-STAT3 than in the ARC (9,13). Thus, while amylin’s role as a leptin sensitizer in the VMN through the STAT3 pathway targets eating preferentially, amylin’s effect on the ERK signaling pathway in ARC neurons might modulate other aspects of energy balance such as energy expenditure and metabolism. Indeed, the depletion of CTR in the VMH of adult DR rats induced increased weight gain and adiposity on a high-fat diet, whereas eating remained unaltered (9), suggesting a critical role for amylin to influence energy expenditure. We next demonstrated that amylin acts preferentially on POMC neurons compared with NPY neurons in adult animals. We postulate that amylin’s rapid action on eating takes place through the AP/NTS pathway (6,35), while amylin’s effect on long-term energy homeostasis acts through ARC

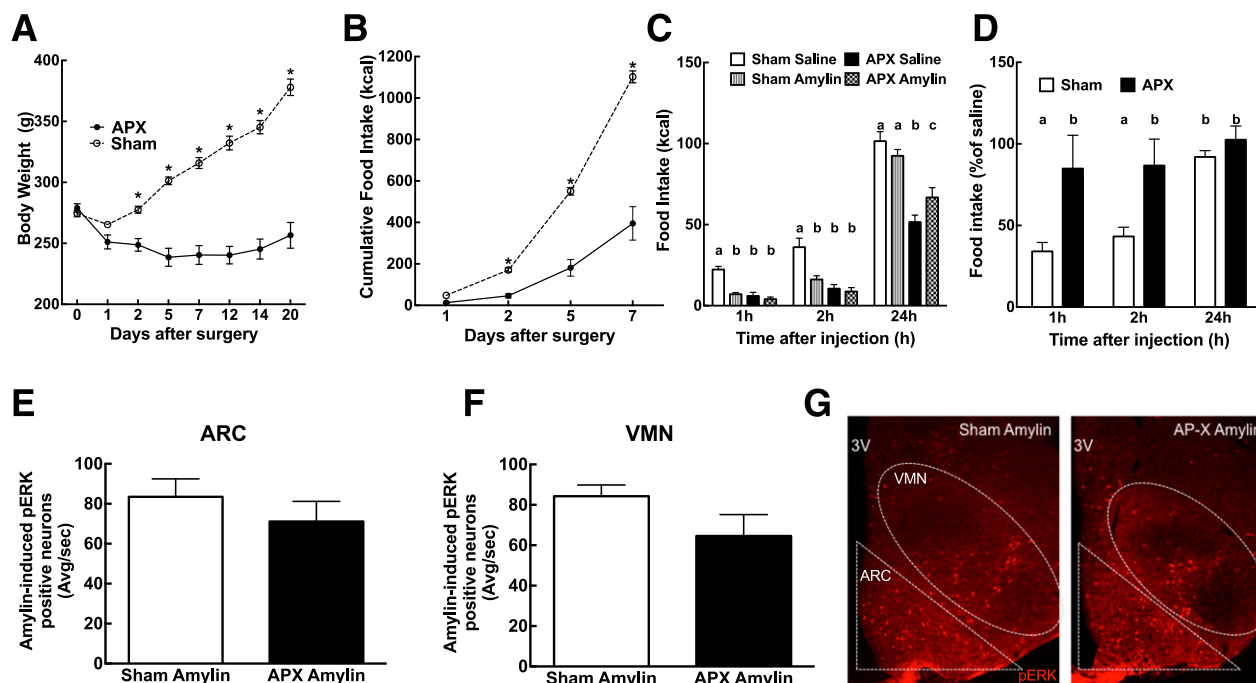


Figure 7—APX lesioning was performed in 6-week-old male Sprague-Dawley rats. Weight (A) and food intake (B), represented as cumulative food intake, were monitored after the surgery. C: Amylin-induced anorexia test was performed after 10 days (20 μ g/kg i.p.), and food intake was measured 1 h and 2 h after injection. D: Food intake after amylin expressed as a percent of baseline. ARC (E) and VMN (F) amylin-induced p-ERK IHC was performed, and positive neurons were counted. G: 10 \times representative picture of the ARC 45 min after amylin injection (50 μ g/kg i.p.) in sham and AP-lesioned (AP-X) rats. p-ERK neurons are in red. $N = 8$ /group. Data are mean \pm SEM. * $P < 0.05$ vs. saline after one-way ANOVA with repeated measures followed by post hoc t test. Parameters with differing superscripts differ from each other at the $P < 0.05$ level by post hoc Bonferroni adjustment after significant intergroup differences were found by two-way ANOVA. 3V, third ventricle; APX, AP-lesioned; Avg/sec, average per section.

POMC neurons similarly to leptin (28). This hypothesis will have to be assessed in future studies.

In the ARC and VMN, amylin is known to synergize with leptin (13), but whether leptin or LepRb is necessary to enhance amylin signaling remains unknown. Our studies confirm that the presence of leptin is not necessary for amylin's acute actions on ARC neurons, whereas the presence of the LepRb, or effects induced by leptin, appear to be critical. Thus, amylin-induced p-ERK was decreased in the ARC of ob/ob mice, suggesting that some leptin or leptin signaling must be present for full amylin action. Indeed, the effect of amylin on p-ERK expression was restored when ob/ob mice were injected with leptin from P4 to P16 to pharmacologically replace leptin during the critical neonatal period (17,54,55). It is important to note that the brains of the respective animals were analyzed 8 days after the last leptin injection, suggesting that leptin per se does not need to be present for amylin to act. Furthermore, amylin-induced p-ERK was decreased in LepRb LoxTB mice. Hence, LepRb seems to be necessary for amylin to activate ARC ERK signaling. Currently, we cannot decipher whether this decrease was due to the absence of LepRb at the time of testing or due to abnormal hypothalamic axonal fiber development that could prevent the action of amylin, similar to what has been shown with leptin (21,56). We hypothesize

that the latter factor may be more important. Indeed, amylin-induced p-ERK signaling in leptin-treated ob/ob mice was completely restored to the level of WT controls, suggesting that once leptin's neurotrophic action took place during the neonatal period, this was sufficient to restore ARC amylin signaling (18).

One drawback of this study is that, since LepRb LoxTB mice were obese once amylin-induced p-ERK was tested, their obesity and its metabolic concomitants could have thus played a role in the absence of an amylin effect on the ERK signaling pathway in the ARC. However, the fact that saline- and leptin-treated ob/ob mice had similar weights, but only leptin-treated mice had amylin-induced p-ERK at this time, supports the hypothesis that amylin's activation of ERK signaling requires leptin, independent of body weight.

While we first focused here only on amylin-induced p-ERK, leptin also activates the MAPK/p-ERK downstream pathway in the ARC which modulates energy expenditure at adulthood (28) and increases ARC projections neonatally (19). Bouret et al. (19) also showed that the disruption of LepRb \rightarrow ERK signaling does not disrupt AgRP and α MSH projection in adult mice as compared with LepRb \rightarrow STAT3 signaling, suggesting the possible action of other neurotrophic factors such as amylin acting to normalize these projections. From this and our previously

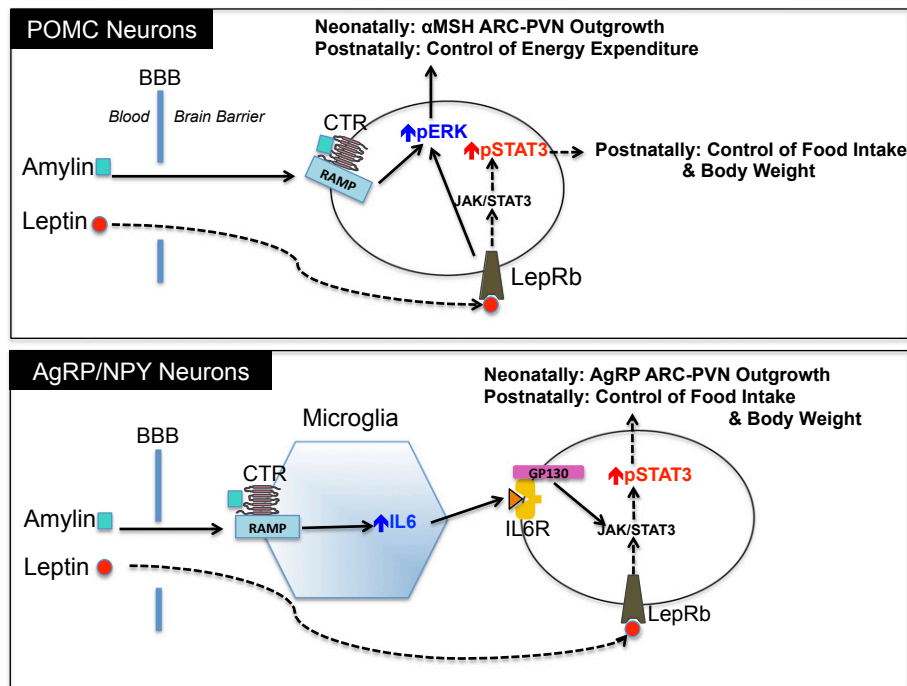


Figure 8—Hypothetical model for mechanisms of amylin and leptin's actions in ARC POMC and AgRP/NPY neurons during the neonatal and adult stage. BBB, blood-brain barrier.

published studies (9), we now confirm that amylin can enhance leptin's neurotrophic action through ERK signaling and that amylin and leptin have an additive effect on activation of the ERK signaling pathway downstream of their respective receptors, similar to the p-STAT3 pathway (13). Moreover, since amylin-induced p-ERK is decreased when LepRb is absent and subthreshold doses of amylin and leptin, which in themselves have no activity, activate ERK signaling when given together, it is likely that leptin and amylin act directly on their respective receptors to codependently activate ERK signaling.

To conclude, while amylin acts indirectly to enhance p-STAT3-mediated leptin signaling in the VMH (10,11,13), the current studies demonstrate the novel finding that amylin directly activates ARC p-ERK signaling, primarily in POMC neurons, as a potential mechanism by which amylin activates these neurons and by which it exerts its neurotrophic properties on α MSH axon outgrowth during postnatal hypothalamic development (Fig. 8).

Acknowledgments. The authors specifically thank Kathleen Caron (University of South Carolina) for supplying the RAMP1/3 KO mice. The authors acknowledge Amylin Pharmaceuticals, Inc., for providing the founders of the authors' amylin KO mouse colony. The AAV CTR shRNA was a gift from Matthew R. Hayes (University of Pennsylvania). The authors gratefully acknowledge the Center for Microscopy and Image Analysis (University of Zurich, Zurich, Switzerland).

Funding. This work was supported by the Swiss National Science Foundation (SNF 31003A_156935 [to T.A.L.]) and by the Research Service of the Department of Veterans Affairs (to A.A.D.-M. and B.E.L.) and the National Institute of Diabetes and Digestive and Kidney Diseases (DK-84142 and DK-102780 [to S.G.B.] and DK-030066 [to B.E.L.]).

Duality of Interest. No potential conflicts of interest relevant to this article were reported.

Author Contributions. T.A.L. and C.L.F. designed the experiments and wrote the manuscript. B.C., L.W., A.A.D.-M., C.N.B., S.G.B., and C.L.F. performed the research and reviewed the manuscript. B.E.L. helped design the experiments and reviewed the manuscript. T.A.L. and C.L.F. are the guarantors of this work and, as such, had full access to all the data in the study and take responsibility for the integrity of the data and the accuracy of the data analysis.

Prior Presentation. Parts of this study were presented in abstract form at the 25th Annual Meeting of the Society for the Study of Ingestive Behavior, Montreal, Canada, 18–22 July 2017.

References

- Ogawa A, Harris V, McCorkle SK, Unger RH, Luskey KL. Amylin secretion from the rat pancreas and its selective loss after streptozotocin treatment. *J Clin Invest* 1990;85:973–976
- Lutz TA. Effects of amylin on eating and adiposity. *Handb Exp Pharmacol* 2012; 209:231–250
- Qi T, Christopoulos G, Bailey RJ, Christopoulos A, Sexton PM, Hay DL. Identification of N-terminal receptor activity-modifying protein residues important for calcitonin gene-related peptide, adrenomedullin, and amylin receptor function. *Mol Pharmacol* 2008;74:1059–1071
- McLatchie LM, Fraser NJ, Main MJ, et al. RAMPs regulate the transport and ligand specificity of the calcitonin-receptor-like receptor. *Nature* 1998;393:333–339
- Hilton JM, Chai SY, Sexton PM. In vitro autoradiographic localization of the calcitonin receptor isoforms, C1a and C1b, in rat brain. *Neuroscience* 1995;69:1223–1237
- Lutz TA, Mollet A, Rushing PA, Riediger T, Scharrer E. The anorectic effect of a chronic peripheral infusion of amylin is abolished in area postrema/nucleus of the solitary tract (AP/NTS) lesioned rats. *Int J Obes Relat Metab Disord* 2001;25:1005–1011
- Riediger T, Schmid HA, Lutz T, Simon E. Amylin potently activates AP neurons possibly via formation of the excitatory second messenger cGMP. *Am J Physiol Regul Integr Comp Physiol* 2001;281:R1833–R1843

8. Riediger T, Zuend D, Becskei C, Lutz TA. The anorectic hormone amylin contributes to feeding-related changes of neuronal activity in key structures of the gut-brain axis. *Am J Physiol Regul Integr Comp Physiol* 2004;286:R114–R122
9. Dunn-Meynell AA, Le Foll C, Johnson MD, Lutz TA, Hayes MR, Levin BE. Endogenous VMH amylin signaling is required for full leptin signaling and protection from diet-induced obesity. *Am J Physiol Regul Integr Comp Physiol* 2016;310:R355–R365
10. Levin BE, Lutz TA. Amylin and leptin: co-regulators of energy homeostasis and neuronal development. *Trends Endocrinol Metab* 2017;28:153–164
11. Roth JD, Roland BL, Cole RL, et al. Leptin responsiveness restored by amylin agonism in diet-induced obesity: evidence from nonclinical and clinical studies. *Proc Natl Acad Sci U S A* 2008;105:7257–7262
12. Turek VF, Trevaskis JL, Levin BE, et al. Mechanisms of amylin/leptin synergy in rodent models. *Endocrinology* 2010;151:143–152
13. Le Foll C, Johnson MD, Dunn-Meynell AA, Boyle CN, Lutz TA, Levin BE. Amylin-induced central IL-6 production enhances ventromedial hypothalamic leptin signaling. *Diabetes* 2015;64:1621–1631
14. Larsen L, Le Foll C, Dunn-Meynell AA, Levin BE. IL-6 ameliorates defective leptin sensitivity in DIO ventromedial hypothalamic nucleus neurons. *Am J Physiol Regul Integr Comp Physiol* 2016;311:R764–R770
15. Padilla SL, Carmody JS, Zeltser LM. Pomc-expressing progenitors give rise to antagonistic neuronal populations in hypothalamic feeding circuits. *Nat Med* 2010;16:403–405
16. Ishii Y, Bouret SG. Embryonic birthdate of hypothalamic leptin-activated neurons in mice. *Endocrinology* 2012;153:3657–3667
17. Bouret SG, Draper SJ, Simerly RB. Formation of projection pathways from the arcuate nucleus of the hypothalamus to hypothalamic regions implicated in the neural control of feeding behavior in mice. *J Neurosci* 2004;24:2797–2805
18. Bouret SG, Draper SJ, Simerly RB. Trophic action of leptin on hypothalamic neurons that regulate feeding. *Science* 2004;304:108–110
19. Bouret SG, Bates SH, Chen S, Myers MG Jr, Simerly RB. Distinct roles for specific leptin receptor signals in the development of hypothalamic feeding circuits. *J Neurosci* 2012;32:1244–1252
20. Levin BE, Dunn-Meynell AA, Balkan B, Keesey RE. Selective breeding for diet-induced obesity and resistance in Sprague-Dawley rats. *Am J Physiol* 1997;273:R725–R730
21. Bouret SG, Gorski JN, Patterson CM, Chen S, Levin BE, Simerly RB. Hypothalamic neural projections are permanently disrupted in diet-induced obese rats. *Cell Metab* 2008;7:179–185
22. Johnson MD, Bouret SG, Dunn-Meynell AA, Boyle CN, Lutz TA, Levin BE. Early postnatal amylin treatment enhances hypothalamic leptin signaling and neural development in the selectively bred diet-induced obese rat. *Am J Physiol Regul Integr Comp Physiol* 2016;311:R1032–R1044
23. Torii S, Nakayama K, Yamamoto T, Nishida E. Regulatory mechanisms and function of ERK MAP kinases. *J Biochem* 2004;136:557–561
24. Chang L, Karin M. Mammalian MAP kinase signalling cascades. *Nature* 2001;410:37–40
25. Nishimoto S, Nishida E. MAPK signalling: ERK5 versus ERK1/2. *EMBO Rep* 2006;7:782–786
26. Yuan LL, Adams JP, Swank M, Sweatt JD, Johnston D. Protein kinase modulation of dendritic K⁺ channels in hippocampus involves a mitogen-activated protein kinase pathway. *J Neurosci* 2002;22:4860–4868
27. Potes CS, Boyle CN, Wookey PJ, Riediger T, Lutz TA. Involvement of the extracellular signal-regulated kinase 1/2 signaling pathway in amylin's eating inhibitory effect. *Am J Physiol Regul Integr Comp Physiol* 2012;302:R340–R351
28. Rahmouni K, Sigmund CD, Haynes WG, Mark AL. Hypothalamic ERK mediates the anorectic and thermogenic sympathetic effects of leptin. *Diabetes* 2009;58:536–542
29. Berglund ED, Vianna CR, Donato J Jr, et al. Direct leptin action on POMC neurons regulates glucose homeostasis and hepatic insulin sensitivity in mice. *J Clin Invest* 2012;122:1000–1009
30. Dackor R, Fritz-Six K, Smithies O, Caron K. Receptor activity-modifying proteins 2 and 3 have distinct physiological functions from embryogenesis to old age. *J Biol Chem* 2007;282:18094–18099
31. Le Foll C, Dunn-Meynell A, Musatov S, Magnan C, Levin BE. FAT/CD36: a major regulator of neuronal fatty acid sensing and energy homeostasis in rats and mice. *Diabetes* 2013;62:2709–2716
32. Le Foll C, Dunn-Meynell AA, Levin BE. Role of FAT/CD36 in fatty acid sensing, energy, and glucose homeostasis regulation in DIO and DR rats. *Am J Physiol Regul Integr Comp Physiol* 2015;308:R188–R198
33. Le Foll C, Corporeau C, Le Guen V, Gouyguou JP, Bergé JP, Delarue J. Long-chain n-3 polyunsaturated fatty acids dissociate phosphorylation of Akt from phosphatidylinositol 3'-kinase activity in rats. *Am J Physiol Endocrinol Metab* 2007;292:E1223–E1230
34. Braegger FE, Asarian L, Dahl K, Lutz TA, Boyle CN. The role of the area postrema in the anorectic effects of amylin and salmon calcitonin: behavioral and neuronal phenotyping. *Eur J Neurosci* 2014;40:3055–3066
35. Lutz TA, Senn M, Althaus J, Del Prete E, Ehrensperger F, Scharrer E. Lesion of the area postrema/nucleus of the solitary tract (AP/NTS) attenuates the anorectic effects of amylin and calcitonin gene-related peptide (CGRP) in rats. *Peptides* 1998;19:309–317
36. Paxinos GF, Franklin KBJ. *Paxinos and Franklin's the Mouse Brain in Stereotaxic Coordinates*. 4th ed. Cambridge, MA, Academic Press, 2012
37. Patterson CM, Bouret SG, Dunn-Meynell AA, Levin BE. Three weeks of postweaning exercise in DIO rats produces prolonged increases in central leptin sensitivity and signaling. *Am J Physiol Regul Integr Comp Physiol* 2009;296:R537–R548
38. Patterson CM, Bouret SG, Park S, Irani BG, Dunn-Meynell AA, Levin BE. Large litter rearing enhances leptin sensitivity and protects selectively bred diet-induced obese rats from becoming obese. *Endocrinology* 2010;151:4270–4279
39. Lee SM, Hay DL, Pioszak AA. Calcitonin and amylin receptor peptide interaction mechanisms: insights into peptide-binding modes and allosteric modulation of the calcitonin receptor by receptor activity-modifying proteins. *J Biol Chem* 2016;291:8686–8700
40. Bouret SG, Bates SH, Kirigiti MA, et al. Leptin promotes formation of projection pathways from the arcuate nucleus of the hypothalamus through activation of ObRb signaling pathways. In *Proceedings of the 34th Annual Meeting of the Society For Neuroscience, San Diego, CA, 2004*. Washington, DC, Society for Neurosciences
41. Potes CS, Lutz TA, Riediger T. Identification of central projections from amylin-activated neurons to the lateral hypothalamus. *Brain Res* 2010;1334:31–44
42. Potes CS, Turek VF, Cole RL, et al. Noradrenergic neurons of the area postrema mediate amylin's hypophagic action. *Am J Physiol Regul Integr Comp Physiol* 2010;299:R623–R631
43. Mercer AJ, Hentges ST, Meshul CK, Low MJ. Unraveling the central proopiomelanocortin neural circuits. *Front Neurosci* 2013;7:19
44. Grove KL, Allen S, Grayson BE, Smith MS. Postnatal development of the hypothalamic neuropeptide Y system. *Neuroscience* 2003;116:393–406
45. Grove KL, Smith MS. Ontogeny of the hypothalamic neuropeptide Y system. *Physiol Behav* 2003;79:47–63
46. Sahu A, Kalra SP, Crowley WR, Kalra PS. Evidence that NPY-containing neurons in the brainstem project into selected hypothalamic nuclei: implication in feeding behavior. *Brain Res* 1988;457:376–378
47. Hay DL, Chen S, Lutz TA, Parkes DG, Roth JD. Amylin: pharmacology, physiology, and clinical potential. *Pharmacol Rev* 2015;67:564–600
48. Kechele DO, Dunworth WP, Trincot CE, et al. Endothelial restoration of receptor activity-modifying protein 2 is sufficient to rescue lethality, but survivors develop dilated cardiomyopathy. *Hypertension* 2016;68:667–677
49. Bachmanov AA, Reed DR, Beauchamp GK, Tordoff MG. Food intake, water intake, and drinking spout side preference of 28 mouse strains. *Behav Genet* 2002;32:435–443
50. Li Z, Kelly L, Heiman M, Greengard P, Friedman JM. Hypothalamic amylin acts in concert with leptin to regulate food intake. *Cell Metab* 2016;23:945

51. Abegg K, Hermann A, Boyle CN, Bouret SG, Lutz TA, Riediger T. Involvement of amylin and leptin in the development of projections from the area postrema to the nucleus of the solitary tract. *Front Endocrinol (Lausanne)* 2017;8:324
52. Clark WR, Rutter WJ. Synthesis and accumulation of insulin in the fetal rat pancreas. *Dev Biol* 1972;29:468–481
53. Lam BYH, Cimino I, Poxel-Wolf J, et al. Heterogeneity of hypothalamic pro-opiomelanocortin-expressing neurons revealed by single-cell RNA sequencing. *Mol Metab* 2017;6:383–392
54. Ahima RS, Hileman SM. Postnatal regulation of hypothalamic neuropeptide expression by leptin: implications for energy balance and body weight regulation. *Regul Pept* 2000;92:1–7
55. Ahima RS, Prabakaran D, Flier JS. Postnatal leptin surge and regulation of circadian rhythm of leptin by feeding. Implications for energy homeostasis and neuroendocrine function. *J Clin Invest* 1998;101:1020–1027
56. Bouret SG, Simerly RB. Minireview: leptin and development of hypothalamic feeding circuits. *Endocrinology* 2004;145:2621–2626